Food Research International 106 (2018) 495–502

Contents lists available at ScienceDirect

Food Research International

journal homepage: www.elsevier.com/locate/foodres

Effects of the gastric juice injection pattern and contraction frequency on the digestibility of casein powder suspensions in an *in vitro* dynamic rat stomach made with a 3D printed model

Xiaoai Zhang[a,d], Zhenkai Liao[a], Peng Wu[b,*], Liding Chen[c,d,**], Xiao Dong Chen[a,d,***]

[a] Department of Chemical Engineering and Biochemical Engineering, College of Chemistry and Chemical Engineering, Xiamen University, Xiamen 361005, China
[b] Centre for Nutrition and Food Sciences, Queensland Alliance for Agriculture and Food Innovation, The University of Queensland, St Lucia 4072, QLD, Australia
[c] College of Life Sciences, The University of Agriculture and Fujian Forestry University, Fuzhou 350002, China
[d] School of Chemical and Environmental Engineering, College of Chemistry, Chemical Engineering and Materials Science, Soochow University, Suzhou 215123, China

ARTICLE INFO

Keywords:
3D-printed rat stomach mold
Gastric secretion pattern
Contraction frequency
Mechanical force
Casein
In vitro digestibility

ABSTRACT

Previously, we have prepared a version of the dynamic *in vitro* rat stomach system (DIVRS-II or Biomimic Rat II). It was constructed and tested by showing similar digestive behaviors with those occurred *in vivo*. In the present work, a 3D-printed plastic mold was employed to create highly repeatable silicone rat stomach model. It has been seen to have shortened the time to handcraft a model like that used in DIVRS-II. The maximum mechanical force of the current stomach model generated by rolling extrusion is found to be more stable probably due to the more uniform wall thickness of the new model. Then the effects of the simulated gastric secretion patterns and contraction frequency of the system on the *in vitro* digestibility of casein powder suspensions were investigated. The results have shown that the location of the gastric secretion injection has an impact on experimental digestibility. The position of rolling-extrusion area, established at the central part of glandular portion (stomach B), displayed the highest digestibility compared to that at the other locations. Furthermore, the extent of digestion was positively correlated with the contraction frequency of the model stomach system, with the maximum frequency of 12 cpm giving the highest digestibility. This highest digestibility is almost the same as the average value found *in vivo*. The better digestive performance produced by optimizing the gastric secretion pattern and contraction frequency may be both resulted from the improved mixing efficiency of the food matrix with digestive juice. This study shows that it is possible to achieve what *in vivo* in a simulated digestion device, which may be used for future food and nutrition studies *in vitro*.

1. Introduction

It is known that stomach, serving as a biochemical reactor, plays a significant role in digestion of foods by mechanically grinding of large food particles into smaller sizes due to gastric peristalsis and various biochemical reactions (Schulze, 2006). Although the *in vivo* trials are relatively accurate ways to study the function of stomach (Gad & Chengelis, 2007), there are still a lot of advantages of the *in vitro* experiments including time-saving and economic as well as no ethical issues (Chen, 2006; Guerra et al., 2012; Ménard et al., 2014; Wickham, Faulks, & Mills, 2009). In the past several decades, many researchers have put in little effort to develop realistic *in vitro* digestion systems to investigate the structural and biochemical changes of foods or medicines during digestion within a gastrointestinal tract (Sun, Lim, Decker, & Mcclements, 2011). The published models are classified into two types in general, namely, static and dynamic models. The static models always imitate the gastrointestinal (GI) tract by means of stirred beaker, head-over-heels mixer or shaking bath where food is incubated for a specific temperature, pH and time in simulate gastric fluids (De, Wouters, Vermeirssen, Boon, & Verstraete, 2011; Molly, Woestyne, & Verstraete, 1993). Due to the oversimplification of the physiological structure of the GI tract, which is inherently quite complicated, the static models fail to mimic the dynamic digestive behaviors and GI transits occurred *in vivo*. Thus the development of dynamic digestion

* Correspondence to: P. Wu, Centre for Nutrition and Food Sciences, Queensland Alliance for Agriculture and Food Innovation, The University of Queensland, St Lucia 4072, QLD, Australia.
** Correspondence to: L. Chen, College of Life Sciences, The University of Agriculture and Fujian Forestry University, Fuzhou 350002, China.
*** Correspondence to: X.D. Chen, School of Chemical and Environmental Engineering, College of Chemistry, Chemical Engineering and Materials Science, Soochow University, Suzhou 215123, China.
E-mail addresses: p.wu@uq.edu.au (P. Wu), chenliding@suda.edu.cn (L. Chen), dong.chen@monash.edu, xdchen@mail.suda.edu.cn (X.D. Chen).

https://doi.org/10.1016/j.foodres.2017.12.082
Received 29 October 2017; Received in revised form 28 December 2017; Accepted 31 December 2017
Available online 04 January 2018
0963-9969/

models is of greater interest with more practical applications. Currently, there are several complicated models reported in literature and publicized commercially, including the TNO gastric model (Cardot, Beyssac, & Alric, 2007; Venema, Havenaar, Minekus, Mcclements, & Decker, 2009; Verwei, Minekus, Zeijdner, Schilderink, & Havenaar, 2016), the human gastric simulator (HGS) (Kong, Oztop, Singh, & Mccarthy, 2011; Kong & Singh, 2010), the dynamic gastric model (DGM) (Wickham et al., 2009; Wickham, Faulks, Mann, & Mandalari, 2012) and the human gastric digestion simulator (GDS) (Kozu et al., 2014). In spite of having superiority in some aspects compared with the static ones, all of those models ignored the influence of geometrical morphology and physiologic structure of stomach on gastric digestion and emptying behaviors (Barros, Retamal, Torres, Zúñiga, & Troncoso, 2016; Chen, 2016). Previously, we have introduced a "near-real" dynamic *in vitro* rat stomach (DIVRS-I) system, which have been validated by showing similar digestive behaviors of casein powder and large raw rice particles with those obtained from *in vivo* experiments (Chen, Wu, & Chen, 2013; Wu, Chen, Wu, & Chen, 2014). It has also been used to study the role of rigid bran layer in contributing to the lower gastric digestion rate in cooked brown rice compared to that in white rice (Wu, Deng, Wu, Dhital, & Chen, 2017b). The gastric morphology and inner structure of the soft-elastic silicone rat stomach model have been proved to significantly impact the digestive efficiency of the casein powder suspensions (Chen et al., 2013). However, the rate of digestion and buffering ability were lower than that found *in vivo* possibly due to the less efficiently mixing and contraction efficiency. Hence, an upgraded version of the rat stomach system, DIVRS-II, has been recently developed. The DIVRS-II system incorporated an additional rolling extrusion movement on the wall of the silicone rat stomach model (Wu, Bhattarai, et al., 2017; Wu, Liao, Luo, Chen, & Chen, 2017c). The digestibility of the casein powder suspensions and raw rice particles in the DIVRS-II at the end of digestion (t = 180 min) were still lower than the average values obtained from *in vivo*, however, they were did significantly improved by 50% and 32%, respectively, compared with the results obtained from the DIVRS-I (Wu, Liao et al., 2017). The DIVRS-II has also been used to study the fate of starch and protein, and the effect of porcine gastric mucin on digesta rheology and gastric emptying rate as well as hydrolysis of macronutrients in control, pectin and mango diets with different dry matter contents (Wu, Bhattarai et al., 2017). Recently, Bhattarai, Dhital, Wu, Chen, and Gidley (2017) used the DIVRS-II to investigate the effect of legume cell walls on the hydrolysis rate and extent of starch and protein in isolated cooked legume cells occurred in the gastric and small intestinal phases. Although the DIVRS-II has been improved significantly in performance, it still has some shortcomings. For example, the silicone rat stomach models of the DIVRS-I and DIVRS-II reported in our previous work were both made totally by hand (Chen et al., 2013), which were time-consuming with relatively high cost, and also resulted in somewhat poor repeatability in making the model. In addition, for the hand-made silicone rat stomach model, the simulated gastric juice were secreted into the stomach model at controlled rates using a syringe pump then divided into four small gastric secretion silicone tubes (internal diameter 1.0 mm) those were inserted at four different locations of the stomach wall. It was assumed that the gastric juice could be uniformly distributed among the four small secretion tubes contributing to a high mixing efficiency between gastric juice and food matrix. However, in fact, we then observed, through visualization experiments using dye-in-water that the gastric juice was not equally distributed in the small tubes. Some bubbles remaining inside of one or two tubes were found commonly which are expected to prevent the gastric juice delivering into the stomach model (results not shown). It was also found that the wrinkles in the model stomach were very useful in quickly distribute the dye. It was thus speculated that a single larger size secretion tube might already achieve similar mixing efficiency, leading to similar digestibility as that using the four tubes as long as the inserted location of the single tube on the silicone stomach wall is proper to promote mixing (results to be shown later in this paper). In the current work, comparative trials of four secretion tubes and one single secretion tube were conducted to test the hypothesis. Besides, it has been reported that the inlet flow position (3 different positions) in a chemical reactor system did influence the mixing efficiency, resulting in different chemical reaction rates (Arratia, Lacombe, Shinbrot, & Muzzio, 2004). Hence, it is of our interest to investigate whether the injection location of the single gastric secretion tube has an effect on the digestive efficiency in the current rat stomach system. This information is expected to help us better understand the mixing mechanism for the gastric juice and food matrix in the model stomach.

To solve the problems mentioned above, in this study 3D printing technology was employed to fabricate the soft-elastic silicone rat stomach model instead of the previously manual method. The 3D printing-based stomach model is expected to save time in the model making and to produce better uniformity of thickness, repeatability and press-resistance compared to that fabricated by hand. The contraction force of the stomach model generated by the current 3D printing-based DIVRS-II was determined.

Furthermore, in the current work, we fabricated six 3D printing-based rat stomach models with the single gastric secretion tube injected at different locations in order to investigate the effect of the distribution of simulated gastric secretion on the digestibility of casein powder suspensions. Besides, the effect of contraction frequency of the current DIVRS-II (also called Biomimic Rat II which has incorporated duodenum and a model intestine system though this addition was not used in the current work) was investigated to find out the optimum digestive conditions and the best digestibility attained was then compared with the previous results obtained from *in vivo* and the DIVRS-I. The results indicated that the digestibility at the optimum conditions (contraction frequency of 12 cpm; secretion location at B; rolling-extrusion area being the central part of the glandular portion (on side a)) is significantly improved, compared with the results obtained from the DIVRS-I throughout the digestion, and it is almost matching that *in vivo* average in the first 120 min. This information has indicated that it is possible to achieve similar digestive efficiency with that *in vivo* by improving the rat stomach system such as the current DIVRS-II and by optimizing the experimental conditions. With the continuous improvement of the DIVRS-II step by step, it is expected to have broader applications in the areas of animal feeding stuff, functional foods, medicines and *etc.* in the future.

2. Materials and method

2.1. Materials

For comparable purpose, the casein powder (purchased from Sigma (C3400, Sigma–Aldrich, the USA)) used as model food in this study was the same as previously used by Chen et al. (2013) and Wu, Liao et al. (2017). The initial particle size of the casein powder was approximately 131.0 ± 14.7 μm.

The simulated saliva and gastric juice were prepared following the method of Wu et al. (2014) and Wu, Liao et al. (2017). Pepsin, mucin, Folin and Ciocalteu's phenol reagent were purchased from Sigma (Sigma–Aldrich, the USA). All the other chemicals were purchased from Sino pharm Chemical Reagent Co., Ltd. (China).

2.2. Model development

The DIVRS-II is mainly composed of a 3D printing-based soft-elastic rat stomach model, a mechanical-electric driving device, a temperature-controlled box and a gastric secretion and emptying device. The fabrication and operation details have been previously reported (Wu, Deng et al., 2017; Wu, Liao et al., 2017c). The fabrication details of the rat stomach models made by 3D printer are described as follows.

2.2.1. Fabrication of the silicone rat stomach model using a 3D printer

In our previous works, the soft-elastic rat stomach model was created using a silicone mold with aid of an actual rat stomach with its inner-surface turned outwards (Chen et al., 2013). A paraffin mold was then created according to the silicone mold and the silicone was smeared on the surface of the paraffin mold by hand to achieve an approximate thick of 1.5 mm at the fore stomach and 2 mm at the glandular portion. The fabricated stomach model possessed similar size, morphology and inner structure as the real rat stomach. However, such handmade method had some drawbacks, *i.e.* time consuming and labor intensive, hard to accurately control the thickness of the smeared silicone thus leading to a relatively poor repeatability of the stomach models.

In this study, the 3D printing technology was employed to fabricate the rat stomach model instead of the previously handmade approach, which could minimize the defects and individual differences in stomach morphology and wall thickness. We firstly established a three-dimensional model of the rat stomach using the specific modeling software of 3D Max according to the physiological dimensions obtained from living rat stomach (Stevens, 1989). The initial step involved in 3D printing was to determine the pattern of mold. In order to simplify the preparing process, the stomach model was divided into two halves called a and b side (Chen, Jayemanne, & Chen, 2012), so the mold was designed in four parts, and the two parts were used to form inner and outer side of "a", another two parts were created for the side "b". The side a and b side was merged to make up the final rat stomach model. Once the four parts of virtual prototype resembling actual rat stomach were obtained, which were used as the mold of the two halves of the rat stomach, the four real prototypes could be generated by 3D printer using Vero White Plus materials. When the mold was prepared, the melted Dragon Skin silicone, which possesses good properties of water insoluble, heat resistant, non-sticking and strong tensile strength (Chen et al., 2012), was used as the material to create the *in vitro* rat stomach. The silicone gel used here was a mixture of gel A and B (Dragon Skin, Rowe Trading Company, Australia) with adequately and equally mixing in quality after debubbling using the vacuum drying oven (DZF-6090, Shanghai). The compounded silica gel was then injected into the 3D-printed mold carefully at the rates controlled by the 3D max software to create the outer and inner surface of the rat stomach model. After the silicone gel was completely cooled down at room temperature (approximately 4–5 h for shaping), each half of the rat stomach model could thus be obtained. The two halves rat stomachs were then combined into a whole soft-elastic rat stomach model after adhering each other using the same silicone gel. In addition, a length of about 10 cm small silicone tube (1 mm, inner diameter) inserted at different locations of the each rat stomach wall (specifically described in Section 2.2.2), was used to simulate the gastric secretion tube. Fig. 1 shows the procedures involved in the formation of the *in vitro* rat stomach model using the 3D printing technology. Fig. 1E shows the ultimate *in vitro* bionic rat stomach model possessing the similar morphological structure and geometrical size to the actual rat stomach (Gärtner, 2003), with wrinkled inner surface at the glandular portion while smooth inner surface at the fore-stomach (Desesso & Jacobson, 2001). The inside volume of the stomach model is approximately 9.0 ± 0.5 mL, with the average thickness of 3 mm, and occupied a box of around 63.3 × 46.9 × 27.0 mm (length × width × height), respectively.

2.2.2. Preparation of the rat stomach models with different injection locations of single gastric secretion tube

Previously, a 4.0 mm internal diameter PVC pipe linked to four small tubes (internal diameter 1.0 mm) was used to deliver the artificial stomach juice into the *in vitro* rat stomach model (Wu et al., 2014, Wu, Deng et al., 2017, Wu, Liao et al., 2017). At the time, we assumed that the simulate gastric juice from the PVC pipe would flow into the 4 small tubes reasonably equably. During the pre-experiments leading to the current work, however, we found that the gastric juice was not equally distributed among the small tubes, with some bubbles remaining inside of one or two tubes that prevented the gastric juice delivering into the stomach model. Also, in the experiments leading to the current one, we did some dye visualization runs, which showed that the wrinkles in the stomach model were highly efficient to distribute the fluid (results not shown here). It was thus naturally proposed that a single small tube might already produce a similar effect of the gastric juice secretion into the stomach if it is located at an appropriate position on the stomach wall. Experimental results showing the comparison between the 4-tube scenario and the one tube are shown in Fig. 6 later on. As mentioned earlier, in this study, we made six silicone stomach models with the single tube inserted at several positions. The details of the inserted locations of the small tube are shown in Fig. 3.

2.3. Measurement of mechanical force produced by the DIVRS-II system

The mechanical force exerted by the DIVRS-II system was determined following the method of Kong and Singh (2010). A thick-walled silicone hollow bulb (diameter 0.5 cm) was attached to a micro digital manometer (HT1890, Xin Site, Shanghai) (Fig. 4) by a silicone tube and a texture analyzer. The bulb filled with water was placed in the side of the glandular portion of the stomach model. When the DIVRS-II was operated, the balloon was worked on with the rolling eccentric wheels to generate a pressure, which could be recorded by the attached manometer. In order to determine the relationship between the pressure and force implemented on the balloon, a texture analyzer equipped with a cylindrical probe (3.5 cm diameter) was applied to compress the bulb attached to the manometer. The pressure was recorded by the micro digital manometer, and the corresponding squeezing force was measured by the texture analyzer simultaneously. The relationship between the recorded pressure and force could thus be obtained. The pressure produced by the DIVRS-II could be then converted to force using the relational expression.

2.4. In vitro digestion of casein suspensions in a single secretion tube device

As mentioned earlier, in order to investigate how the distributions of gastric secretion tube affects the digestive performance, six silicone stomach models with different secretion locations of the single gastric secretion tube were used for the *in vitro* digestion of the casein powder suspensions. For each rat stomach model, the digestion procedure was almost the same as what had been reported by Chen et al. (2013). Initially, 0.6 mL simulated gastric juice which have been preheated to 37 °C was injected into the 3D printing-based silicone rat stomach model to mimic the fast state before the food loading. The food sample (0.3 g casein particles mixed with 4 mL deionized water) was then fed to the model stomach through the model esophagus. A syringe pump was used to deliver the simulated gastric juice into the stomach model through the single small silicone tube (internal diameter 1 mm). The gastric emptying rate of the digesta was controlled by another syringe pump connected by a silicone tube (internal diameter 3 mm) with the model pylorus tube. The driving device was set to create 2.5 compressions and 3 extrusions per minute, and the amplitude of the angled plate was set at 2.6 mm (Chen et al., 2013). The mean rates of gastric juice secretion and the emptying were 25 μL/min and 22 μL/min, respectively, which were determined in agreement with the *in vivo* data reported by Chen et al. (2013). The casein powder suspension was digested continuously in the DIVRS-II for 180 min. For every 30 min, the emptied digesta was collected in a 1.5 mL centrifuge tube. The concentration of soluble peptides in the gastric digesta was determined after centrifuging for solid-liquid separation using the Lowry method (Lowry, Rosebrough, Farr, & Randall, 1951; Peterson, 1979). The gastric secretion position with the highest digestive efficiency in the end of digestion was recognized as the optimal position. The environmental temperature of simulated digestion process was kept at 37 °C by means of the temperature-controlled box. Each digestion test was performed in

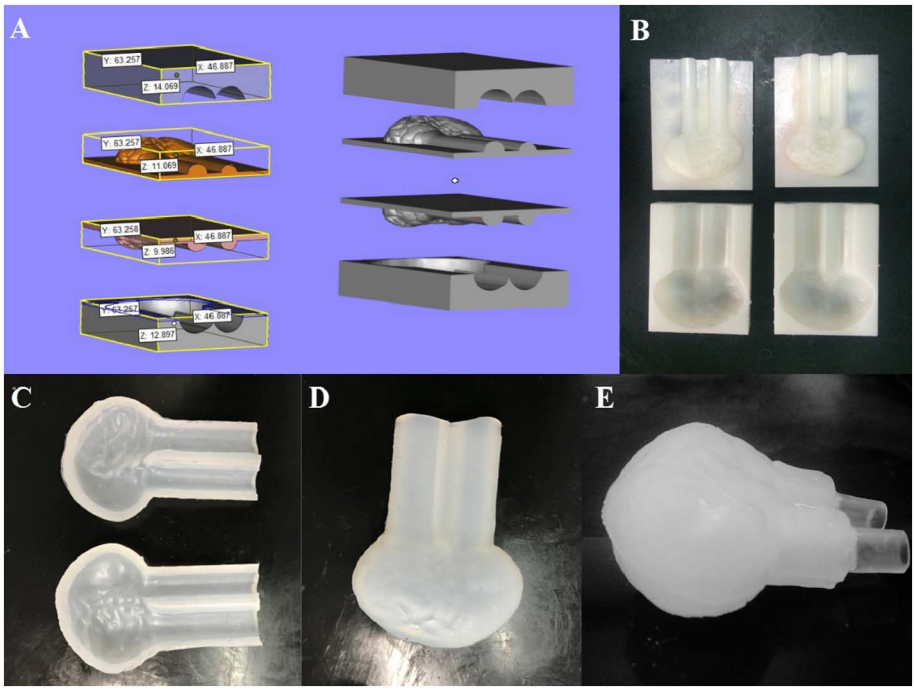

Fig. 1. Fabrication of the silicone rat stomach model using the 3D printing technology. A: Virtual prototype, B: 3D printed rat stomach mold, C: two halves silicone rat stomach, D: semi-finished silicone rat stomach model. E: finished silicone rat stomach.

triplicate.

2.5. Digestion of the casein powder suspensions with different contraction frequencies in the same stomach model

The rat stomach model with the optimal inserted location of the single gastric secretion tube (based on the results obtained in Section 2.4) was used here to investigate the rolling extrusion frequency (3, 6 and 12 cpm) of the driving device on the digestive efficiency of the casein powder suspensions. The specific operations were the same as described in Section 2.4. The frequency where the highest digestibility was obtained was recorded as the optimal digestive condition. The results obtained under the optimal conditions were also compared with those previously reported *in vivo* and *in vitro* rat stomach systems to test how the current DIVRS-II system resembles to the *in vivo*.

2.6. Statistical analysis

All experiments were carried out in triplicate using the same food sample during the comparison trials and all results were expressed as the means ± standard deviation. A significance test was conducted using one-way analysis of variance (ANOVA) to analyze the digestibility of casein powder suspensions at the end of digestion (t = 180 min) when comparing with the previously published data obtained from the *in vivo* and *in vitro*. Statistical significance was set at a probability level of 0.05. The coefficient of variation (CV) was calculated as a percentage of the standard deviation to the mean value (SD/mean × 100) and was used to evaluate the repeatability of the stomach models.

3. Results and discussion

3.1. Measurement of the overall contraction force

As it is shown in Fig. 5A, a linear relationship between the pressure and force could be obtained using the texture analyzer. According to the linear equation, the pressure data of the DIVRS-II contraction recorded by the manometer could be then converted to force. Fig. 5B presents the change in the contraction force produced by the rolling extrusion on the stomach wall, with the maximum force of 4.20 ± 0.09 N when the two rollers approached each other at the minimum distance of 8.5 mm. It is noted that the maximum force is significantly higher than that has been reported *in vivo* trials on living rats showing the dominant contraction force of 2.26 ± 1.42 g generated by the peristaltic contraction. A higher contraction force applied in the DIVRS-II was expected to

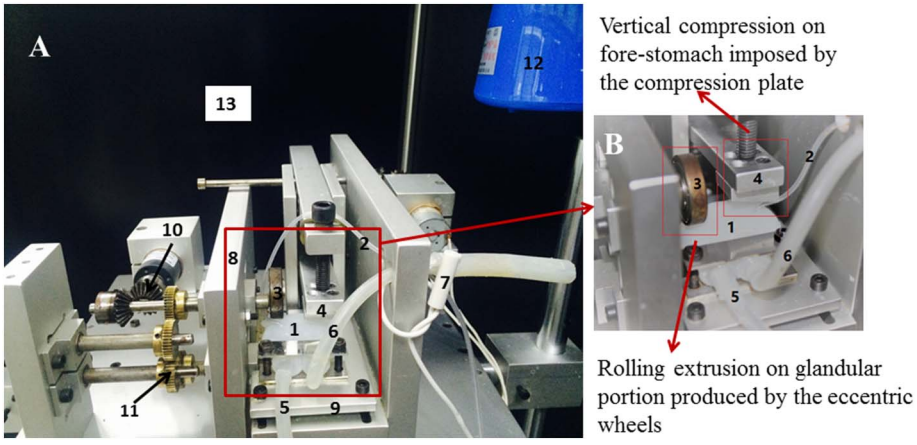

Fig. 2. Updated version of the dynamic *in vitro* rat stomach system (DIVRS-II). Fig. 2B is a local magnification of Fig. 2A showing the two different types of movements implemented on the wall of the 3D-printed *in vitro* soft rat stomach. (1) 3D-printed silicone rat stomach model; (2) gastric juice secretion tube; (3) eccentric wheel; (4) compression plate; (5) emptying tube; (6) model esophagus; (7) thermocouple; (8) fixed plate; (9) aluminum base plate; (10) bevel gear; (11) gear; (12) heat preservation lamp; (13) temperature-controlled box.

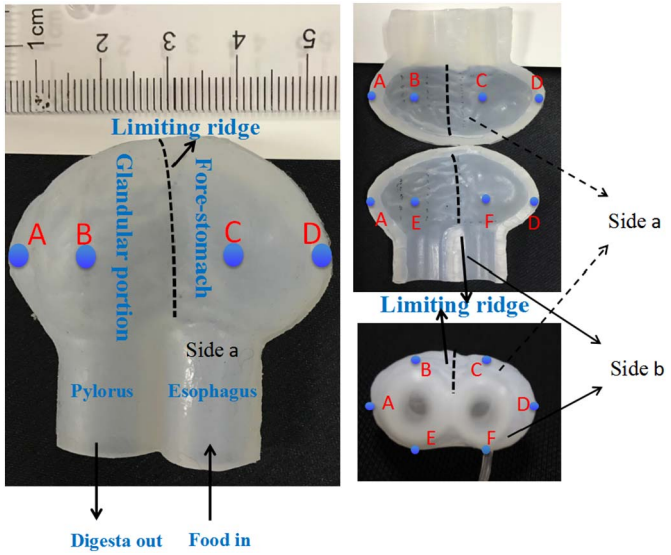

Fig. 3. The six silicone rat stomach models showing the details of inserting locations of the single gastric secretion tube on the stomach wall. Different letters represent different inserting locations of each stomach model. Stomach A: edge of glandular portion (the central part) (junction of side a and b); stomach B: rolling-extrusion area (the central part) of glandular portion (side a); stomach C: compression area (the central part) of forestomach (side a); stomach D: edge of forestomach (the central part) (junction of side a and b); stomach E: rolling-extrusion area (the central part) of glandular portion (side b); stomach F: compression area, *i.e.* the central part of forestomach (side b). The letters of "a" and "b" indicate the two sides of the stomach model.

Fig. 4. Mechanical force measuring device, which is composed of a 0.5 cm silicone hollow sphere and a digital manometer.

produce higher mixing and grinding efficiency thus contributing to higher digestibility of the food matrix. In addition, the maximum compressive force generated by the previous DIVRS-I was 5.87 N (Chen et al., 2013), a little higher compared to the DIVRS-II due to the different fabrication methods of the stomach model. In addition, there are no significant differences in the compression force among different compression locations of the stomach wall. This result may suggest that DIVRS-II with 3D printing-based silicone rat stomach model has better stress resistance (Chen et al., 2013) probably benefiting from the uniform thickness of the stomach model that was made using the 3D-printed method.

3.2. Effect of inserting locations of the single gastric secretion tube on digestibility of casein suspensions

Fig. 6 shows the comparative results using the four secretion tubes and the one with the single secretion tube at the optimal location (data to be shown in Fig. 7). This illustrates that one single secretion tube can indeed make the same or similar digestibility of the casein suspensions as that with the four secretion tubes. Based on this finding, the following digestion experiments were all conducted using the 3D printing-based stomach model with single secretion tube.

Fig. 7 shows the changes in the hydrolysis product (soluble peptides) concentration of the casein powder suspensions with respect to digestion time in the current DIVRS-II with varying injection locations of the single gastric secretion tube at the 3D printing-based rat stomach models. The results show that the overall digestion trends are similar among the six stomach models with different gastric juice secretion locations, with the concentration of soluble peptides continuously increasing throughout the digestion time in the DIVRS-II because of the protein was degradation by the digestive enzyme-pepsin (Malito, Hulse, & Tang, 2008; Schmelzer et al., 2007; Umbach, Teschemacher, Praetorius, Hirschhäuser, & Bostedt, 1985). This trend is in agreement with the results previously reported by Chen et al. (2013) and Wu, Liao, et al. (2017). However, due to the injection point for the reactants of chemical reaction influencing the mixing process (Bujalski, Jaworski, Bujalski, & Nienow, 2002; Bulnes-Abundis & Alvarez, 2013), the extents of the digestion of the casein suspensions were different among the locations of the single gastric tube tested. As shown in Fig. 7, the stomach B (rolling-extrusion area being the central part of glandular portion, side a) displayed the highest concentration of the soluble peptides, while the stomach F (compression area being the central part of the forestomach, side b) showed the lowest values during the digestion. This variation indicates that the inserting location of the single gastric tube played an important role in the digestive efficiency of the casein suspensions, which was perhaps due to the different mixing efficiency between the food sample and digestive juice caused by the different secretion locations of the gastric juice through the single tube. Fig. 8 presents the distributions of red food coloring in the rat stomach B and F during digestion. With the same amount of the addition of the red food coloring into the stomach models, the coloring in the stomach B with the gastric tube inserted at the glandular portion was visually uniformly distributed in the whole stomach immediately after 60 min digestion, however, it was inhomogeneously mixed in the stomach F throughout the digestion time. This indicates that the rolling extrusion at the glandular portion could possibly contribute to a better mixing efficiency between the food samples and digestive juice than that at the location F.

3.3. Effect of contraction frequency on digestibility of the casein suspensions

Based on the results obtained in Section 3.2, the rat stomach B with the single gastric secretion tube inserted at the location B (rolling-extrusion area being the central part of glandular portion, side a), which represented the optimal injected location of the gastric juice secretion, was used to study the effect of rolling extrusion frequency on the digestibility of the casein suspensions in the DIVRS-II system (Haba & Sarna, 1993). Fig. 9 shows the change in the concentration of soluble peptides during gastric digestion in the DIVRS-II at the contraction frequency of 3, 6 and 12 cpm. With the increase of the rolling extrusion frequency from 3 to 6 cpm, the digestion extent of the casein suspensions as expressed by the concentration of the soluble peptides was slightly increased throughout the whole time. However, when the frequency increased to 12 cpm, the extent of digestion was significantly increased at each time point compared to the frequencies at 3 and 6 cpm. This was perhaps due to the improved mixing efficiency between the food sample and digestive juice that contributed to the higher digestive efficiency.

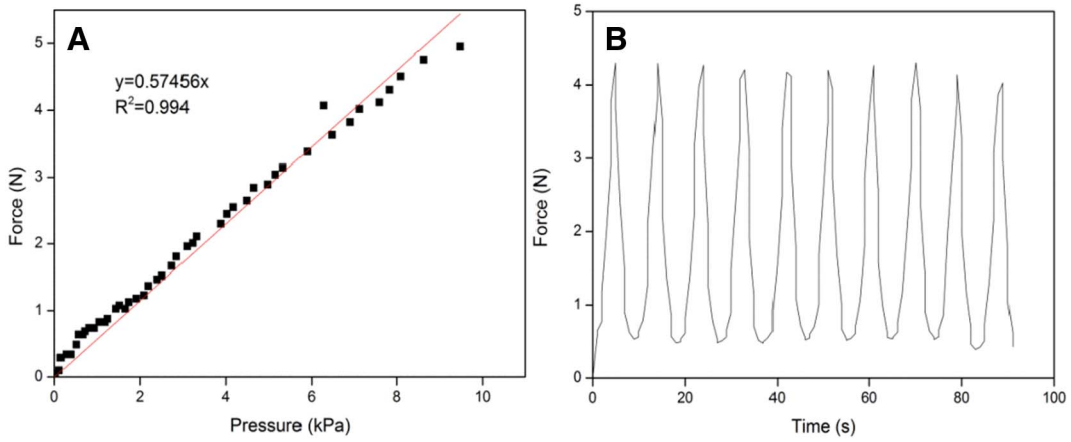

Fig. 5. Linear relationship between the pressure inside the balloon measured by a digital manometer and the force applied on the silicone bulb measured by a texture analyzer (A); profile of contraction force applied on the 3D-printing based silicone rat stomach model produced by the DIVRS-II (B).

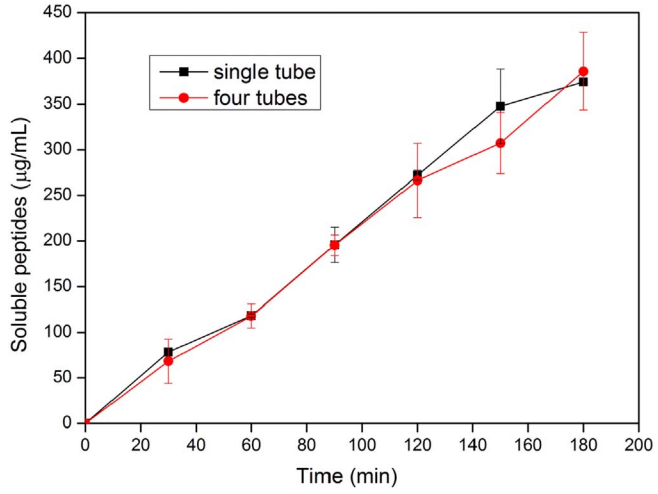

Fig. 6. Changes in the concentration of soluble peptides of the gastric digesta of the casein suspensions during gastric digestion in the different *in vitro* rat stomach models with different quantity secretion tube. Experimental conditions are the same as the description of the Section 2.4.

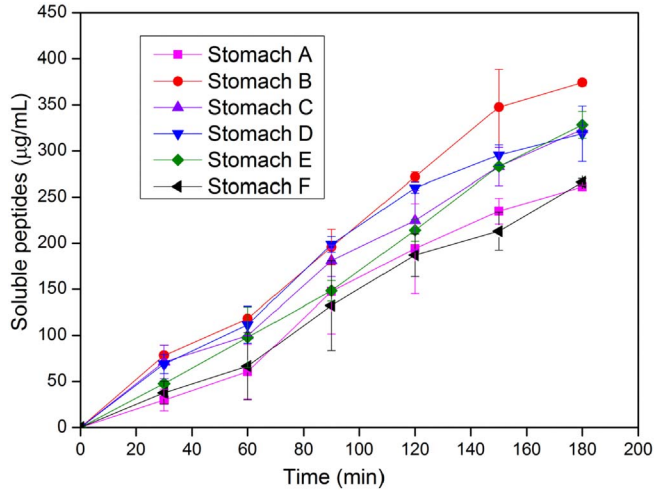

Fig. 7. Changes in the concentration of soluble peptides of the gastric digesta of the casein suspensions during gastric digestion in the different *in vitro* rat stomach models with different injection locations of the single gastric secretion tube. The different letters represent different artificial gastric juice injection locations, which are the same as described in Fig. 3.

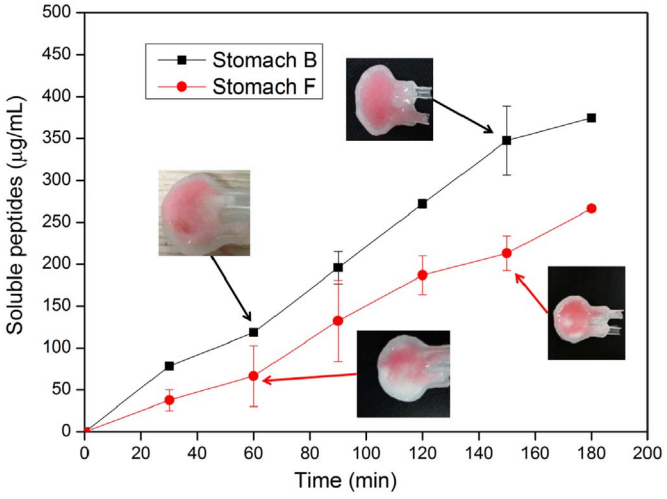

Fig. 8. The distributions of red food coloring in the rat stomach B and F during digestion. Stomach B: the single gastric tube was inserted at the rolling-extrusion area, *i.e.* the central part of glandular portion (side a); stomach F: the single gastric tube was inserted at the compression area (the central part) of forestomach (side b). (For interpretation of the references to colour in this figure legend, the reader is referred to the web version of this article.)

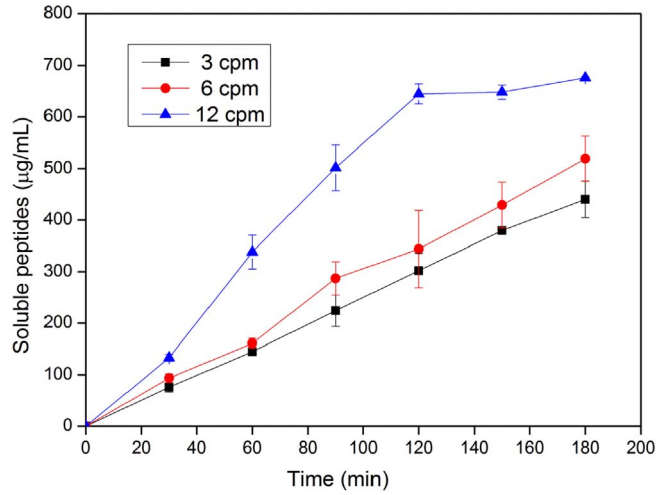

Fig. 9. Concentration of soluble peptides during gastric digestion in the DIVRS-II at the contraction frequency of 3, 6 and 12 cpm.

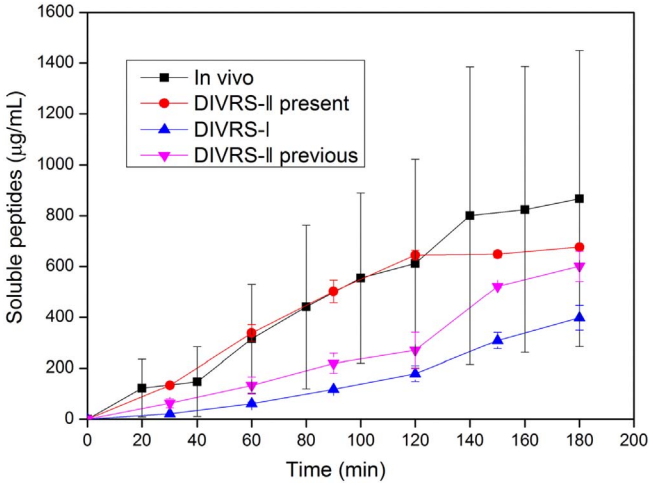

Fig. 10. Soluble peptides of the gastric digesta of the casein suspensions during gastric digestion in the *in vivo*, DIVRS-I, previous DIVRS-II and present DIVRS-II. The data of the *in vivo*, DIVRS-I and previous DIVRS-II shown here are cited from previously published work (Chen et al., 2013; Wu, Bhattarai, et al., 2017).

3.4. Comparison of digestibility between in vitro and in vivo stomach systems

For comparable purpose to test the digestive capacity of the present DIVRS-II system with the rat stomach model made by 3D printer (at the optimal digestion conditions: frequency of 12 cpm and stomach B with the gastric juice secretion at location B), the previously published results obtained from the *in vivo* of living rats, DIVRS-I and previous version of the DIVRS-II (as stated above, the rat stomach model was made by hand and the rolling extrusion frequency was 3 cpm) are all displayed in Fig. 10, showing the change in the concentration of soluble peptides with respect to digestion time during digestion. The details of the *in vivo* experiments and *in vitro* tests in the DIVRS-I and DIVRS-II had been clearly presented in our previous work (Chen et al., 2013; Wu, Liao, et al., 2017). For easy reading, they have also been included in the Supporting Information. As presented in Fig. 10, the present DIVRS-II shows consistent digestion profile of the casein suspensions with the other stomach systems, with the soluble peptides concentration increasing with digestion time. The peptide concentration *in vivo* displayed no significant difference ($p > 0.05$) at each time point before 120 min compared to that in the present DIVRS-II, whereas it was significantly higher than that in the DIVRS-I and previous DIVRS-II systems ($p < 0.05$). At the digestion time point of 120 min, the concentration of the soluble peptides in the present DIVRS-II reached up to 600 μg/mL, which was approximately 3 times higher than that in the previous DIVRS-II and was already very close to that found *in vivo*. In the later stage of digestion between 120 min and 180 min, the extent of digestion in the present DIVRS-II kept continuously increasing although the digestion rate was relatively decreased. At the end of digestion (180 min), the concentration of the soluble peptides was 676 ± 2 μg/mL in the present DIVRS-II, which was still a little lower compared to that *in vivo* (867 ± 582 μg/mL) but no significant difference was observed ($p > 0.05$). These results indicate that the conversion efficiency was remarkably improved in the present DIVRS-II system, which was mainly due to the fact that the 3D-printed rat stomach model and the larger frequency of the rolling extrusion could generate higher grinding force and better mixing efficiency between the casein particles and digestive juice. In addition, the CV of the data of the concentration of soluble peptides, calculated as the ratio of the standard deviations to the arithmetic mean, is generally within 5% in the present DIVRS-II, whereas about 10% in the previous DIVRS-II and DIVRS-I, and up to 70% *in vivo*, indicating an improvement of repeatability in the previous DIVRS-II compared to the other stomach systems.

4. Conclusions

We introduced the 3D printing technology to prepare the soft-elastic silicone rat stomach model instead of the previously manual method for the previous DIVRS-II system. The 3D printing-based stomach model had better reproducibility of digestion tests probably benefiting from its more uniform thickness. The simulated gastric secretion distribution pattern could affect the digestibility of the casein suspensions during digestion, with the position of rolling-extrusion area being at the central part of glandular portion (stomach B) producing the highest digestibility compared to the other locations. Furthermore, the digestibility has been found to be positively correlated with the contraction frequency of the stomach system, with the frequency of 12 cpm performing the best digestibility. The extent of digestion of the casein suspensions was significantly increased in the current DIVRS-II system (Biomimic Rat II) under the optimal conditions with the single gastric tube inserted at location B and the rolling extrusion frequency of 12 cpm, compared to the DIVRS-I and previous DIVRS-II systems, attained even closer results to that *in vivo*. This indicates that it is highly feasible to achieve similar digestive efficiency of the casein suspensions as that obtained *in vivo* by optimizing the fabrication methods of the silicone stomach model, and by selecting appropriate contraction frequency. Future plans will focus on further improving the present system to investigate the appropriate behaviors of the duodenum and the simulated intestine, and make it more automated and intelligent for the ease of operations.

Acknowledgements

This work was supported by the National Natural Science Foundation of China - the Optimized Research on *In Vitro* Soft-elastic Rat Stomach Biomimetic Digestive System (general program, No. 21676172).

Appendix A. Supplementary data

Supplementary data to this article can be found online at https://doi.org/10.1016/j.foodres.2017.12.082.

References

Arratia, P. E., Lacombe, J. P., Shinbrot, T., & Muzzio, F. J. (2004). Segregated regions in continuous laminar stirred tank reactors. *Chemical Engineering Science, 59*(7), 1481–1490.

Barros, L., Retamal, C., Torres, H., Zúñiga, R. N., & Troncoso, E. (2016). Development of an *in vitro* mechanical gastric system (IMGS) with realistic peristalsis to assess lipid digestibility. *Food Research International, 90*, 216–225.

Bhattarai, R. R., Dhital, S., Wu, P., Chen, X. D., & Gidley, M. J. (2017). Digestion of isolated legume cells in a stomach-duodenum model: Three mechanisms limit starch and protein hydrolysis. *Food & Function, 8*(7), 2573–2582.

Bujalski, J. M., Jaworski, Z., Bujalski, W., & Nienow, A. W. (2002). The influence of the addition position of a tracer on CFD simulated mixing times in a vessel agitated by a rushton turbine. *Chemical Engineering Research and Design, 80*(8), 824–831.

Bulnes-Abundis, D., & Alvarez, M. M. (2013). The simplest stirred tank for laminar mixing: Mixing in a vessel agitated by an off-centered angled disc. *AICHE Journal, 59*(8), 3092–3108.

Cardot, J. M., Beyssac, E., & Alric, M. (2007). In vitro–in vivo correlation: importance of dissolution in IVIVC. *Dissolution Technologies, 14*(1), 15–19.

Chen, X. D. (2006). GIT physicochemical modeling - a critical review. *International Journal of Food Engineering, 2*(4), 88–91.

Chen, X. D. (2016). Scoping biology-inspired chemical engineering. *Chinese Journal of Chemical Engineering, 24*(1), 1–8.

Chen, L., Jayemanne, A., & Chen, X. D. (2012). Venturing into *in vitro* physiological upper GI system focusing on the motility effect provided by a mechanised rat stomach model. *Food Digestion, 4*(1), 36–48.

Chen, L., Wu, X., & Chen, X. D. (2013). Comparison between the digestive behaviors of a new in vitro rat soft stomach model with that of the *in vivo* experimentation on living rats – Motility and morphological influences. *Journal of Food Engineering, 117*(2), 183–192.

De, B. P., Wouters, R., Vermeirssen, V., Boon, N., & Verstraete, W. (2011). Development of a six-stage culture system for simulating the gastrointestinal microbiota of weaned infants. *Microbial Ecology in Health and Disease, 13*(2), 111–123.

Desesso, J. M., & Jacobson, C. F. (2001). Anatomical and physiological parameters

affecting gastrointestinal absorption in humans and rats. *Food and Chemical Toxicology: An International Journal Published for the British Industrial Biological Research Association, 39*(3), 209–228.
Gad, S. C., & Chengelis, C. P. (2007). *Animal models in toxicology. 45 (11)*, CRC/Taylor & Francis239–248.
Gärtner, K. (2003). The forestomach of rats and mice, an effective device supporting digestive metabolism in muridae: A review. *Journal of Experimental Animal Science, 42*(1), 1–20.
Guerra, A., L., E.-M., Livrelli, V., Denis, S., Blanquet-Diot, S., & Alric, M. (2012). Relevance and challenges in modeling human gastric and small intestinal digestion. *Trends in Biotechnology, 30*(11), 591–600.
Haba, T., & Sarna, S. K. (1993). Regulation of gastroduodenal emptying of solids by gastropyloroduodenal contractions. *American Journal of Physiology, 264*(2 Pt 1), G261.
Kong, F., Oztop, M. H., Singh, R. P., & Mccarthy, M. J. (2011). Physical changes in white and brown rice during simulated gastric digestion. *Journal of Food Science, 76*(6), E450–E457.
Kong, F. B., & Singh, R. P. (2010). A human gastric simulator (HGS) to study food digestion in human stomach. *Journal of Food Science, 75*(9), E627–E635.
Kozu, H., Nakata, Y., Nakajima, M., Neves, M. A., Uemura, K., Sato, S., ... Ichikawa, S. (2014). Development of a human gastric digestion simulator equipped with peristalsis function for the direct observation and analysis of the food digestion process. *Food Science and Technology Research, 20*(2), 225–233.
Lowry, O. H., Rosebrough, N. J., Farr, A. L., & Randall, R. J. (1951). Protein measurement with the Folin phenol reagent. *Journal of Biological Chemistry, 193*(1), 265.
Malito, E., Hulse, R. E., & Tang, W.-J. (2008). Amyloid β-degrading cryptidases: Insulin degrading enzyme, presequence peptidase, and neprilysin. *Cellular and Molecular Life Sciences, 65*(16), 2574–2585.
Ménard, O., Cattenoz, T., Guillemin, H., Souchon, I., Deglaire, A., Dupont, D., & Picque, D. (2014). Validation of a new *in vitro* dynamic system to simulate infant digestion. *Food Chemistry, 145*(145C), 1039–1045.
Molly, K., Woestyne, M. V., & Verstraete, W. (1993). Development of a 5-step multi-chamber reactor as a simulation of the human intestinal microbial ecosystem. *Applied Microbiology and Biotechnology, 39*(2), 254.
Peterson, G. L. (1979). Review of the Folin phenol protein quantitation method of Lowry, Rosebrough, Farr and Randall. *Analytical Biochemistry, 100*(2), 201–220.
Schmelzer, C. E., Schöps, R., Reynell, L., Ulbrich-Hofmann, R., Neubert, R. H., & Raith, K. (2007). Peptic digestion of beta-casein. Time course and fate of possible bioactive peptides. *Journal of Chromatography. A, 1166*(1–2), 108.
Schulze, K. (2006). Imaging and modelling of digestion in the stomach and the duodenum. *Neurogastroenterology and Motility, 18*(3), 172–183.
Stevens, C. E. (1989). Comparative physiology of the vertebrate digestive system. *Gut, 30*(7), 1029.
Sun, J. H., Lim, B. O., Decker, E. A., & Mcclements, D. J. (2011). *In vitro* human digestion models for food applications. *Food Chemistry, 125*(1), 1–12.
Umbach, M., Teschemacher, H., Praetorius, K., Hirschhäuser, R., & Bostedt, H. (1985). Demonstration of a β-casomorphin immunoreactive material in the plasma of newborn calves after milk intake. *Regulatory Peptides, 12*(3), 223.
Venema, K., Havenaar, R., Minekus, M., Mcclements, D. J., & Decker, E. A. (2009). Improving in vitro simulation of the stomach and intestines. *Designing Functional Foods. 8 (7). Designing Functional Foods* (pp. 314–339).
Verwei, M., Minekus, M., Zeijdner, E., Schilderink, R., & Havenaar, R. (2016). Evaluation of two dynamic *in vitro* models simulating fasted and fed state conditions in the upper gastrointestinal tract (TIM-1 and tiny-TIM) for investigating the bioaccessibility of pharmaceutical compounds from oral dosage forms. *International Journal of Pharmaceutics, 498*(1–2), 178.
Wickham, M. J. S., Faulks, R. M., Mann, J., & Mandalari, G. (2012). The design, operation, and application of a dynamic gastric model. *Dissolution Technologies, 19*(3), 15–22.
Wickham, M., Faulks, R., & Mills, C. (2009). *In vitro* digestion methods for assessing the effect of food structure on allergen breakdown. *Molecular Nutrition & Food Research, 53*(8), 952–958.
Wu, P., Bhattarai, R. R., Dhital, S., Deng, R., Chen, X. D., & Gidley, M. J. (2017). *In vitro* digestion of pectin- and mango-enriched diets using a dynamic rat stomach-duodenum model. *Journal of Food Engineering, 202*, 65–78.
Wu, P., Chen, L., Wu, X., & Chen, X. D. (2014). Digestive behaviours of large raw rice particles *in vivo* and *in vitro* rat stomach systems. *Journal of Food Engineering, 142*, 170–178.
Wu, P., Deng, R., Wu, X., Dhital, S., & Chen, X. D. (2017). *In vitro* gastric digestion of cooked white and brown rice using a dynamic rat stomach model. *Food Chemistry, 237*, 1065–1072.
Wu, P., Liao, Z., Luo, T., Chen, L., & Chen, X. D. (2017). Enhancement of digestibility of casein powder and raw rice particles in an improved dynamic rat stomach model through an additional rolling mechanism. *Journal of Food Science, 82*, 1387–1394.